Geneid *et al.*
Journal of Engineering and Applied Science (2022) 69:90
https://doi.org/10.1186/s44147-022-00150-z

Journal of Engineering and Applied Science

RESEARCH Open Access

Multi-objective optimization of vertical-axis wind turbine's blade structure using genetic algorithm

Ahmed Ali Geneid[1], Mostafa R. A. Atia[2] and Ahmed Badawy[3*]

*Correspondence: ahbadawy@msa.edu.eg

[1] Ain Shams University, Cairo, Egypt
[2] Arab Academy for Science, Technology and Maritime Transport, Cairo, Egypt
[3] October University for Modern Sciences and Arts MSA, Giza, Egypt

Abstract

Through the field of renewable energy, the vertical-axis wind turbine is preferable, especially when the wind speed is low to medium. The optimization of blade structure design is essential to enhance the usability of the vertical-axis wind turbine. This paper introduces an optimization approach for the uniform blade structure design used in the vertical-axis wind turbine. The blade cost represents 20% of the turbine overall cost, and inertia load is the dominating design load. This approach aims to optimize the weight and the cost while maintaining structural integrity. Designs of blade structure are based on a multi-objective model, including the composite material and geometric parameters, where multiple design parameters are included. The model enhances the requirement of computation time and resources by approximation cross-sectional properties and loading calculations. The cost index concept is investigated to introduce an efficient method for approximation, normalizing the cost from currency exchange and price changes. The formulated model is then validated using a finite element analysis package, where the model is the integration between the numerical geometric model and the classical laminate theory. Optimization models are then formulated based on genetic algorithm and Pareto frontier analysis. Blade design parameters are included in the optimization to cover a wide range of parameters. The geometric cross-sectional properties are estimated using empirical formulas to reduce computation time and resources. The presented approach augmented the blade design parameters and genetic algorithm optimization. Optimum results for NACA 0021 shows the blade mass range between 2.5 and 3 kg and the cost index from 40 to 90.

Keywords: Sustainable design, Genetic algorithm, Multi-objective optimization, Vertical wind turbines, Wind turbine blade structure

Introduction

The concepts of low-speed, noise, independent of wind direction, as well as an economic perspective, are among the reasons for deploying vertical wind turbine (VAWT). Efficient deployment of a VAWT remains in the low-speed wind, which is a crucial advantage over horizontal wind turbines (HAWT). Another beneficial advantage of VAWT is the acceptance of the wind from any direction; besides, the production of VAWT is simpler than HAWT. These advantages make VAWT more adequate for deploying on

the building rooftop and small-scale entities. The rooftop affects the choice of wind turbine type because the shape impacts the airflow above the buildings. HAWT is better for doom and flat roofs; otherwise, VAWT is preferred [1–3]. Moreover, the VAWT has a lower sound level while operation compared to HAWT. Different types of VAWT exist including the Darrieus, H-rotor, and the Savonius. The H-VAWT is a better economic choice in comparison to Darrieus VAWT due to the simplicity of structure and no need for pitch or gearbox mechanisms [4]. Economist recommendation is focusing on optimization of wind turbines design aspects including size, blade material, control devices, forecasting techniques, and financial funds. Besides, the contribution of the rotor blade cost to overall cost is 22% as estimated in [5]. Hence, the blade design becomes the concern of diverse scientific fields, including structural design, aerodynamic analysis, airfoil, and material selection, additionally optimization approaches.

The blade inertia has a higher contribution to the blade deformation compared to aerodynamic loads at the normal working speed [6]. The rigid/flexible nonlinear model investigates the blade's structural dynamic behavior in unsteady wind conditions. The models state that the structural design of the blade should consider the dynamic stiffening effect. Moreover, the structure could be manufactured from short fiber composite material as it has a different behavior compared to the continuous fiber material [7]. The simulation of VAWT in unsteady wind conditions needs further intention, especially in conditions that could affect the structure behavior leading to catastrophic sudden failure. Optimizing the fiber orientation angle and the strength to weight ratio, where a 90° is recommended to reduce the maximum stress and deflection [8].

Design load cases depend on operational and external conditions. The requirements recommended by IEC61400-1 and Germanischer Lyoyd (GL) for the HAWT are unsuitable to VAWT. The ultimate strength analysis is considered for both regular and extreme conditions. However, the fatigue analysis depends only on the regular conditions, since the extreme conditions rarely occur [9]. Other working conditions that should be included are a startup, normal shutdown, and emergency stop. Furthermore, numerical analysis of VAWT H-rotor blade structure against the extreme operating conditions stated in IEC standards to determine the material that could support the maximum load [10].

The optimization of the vertical wind turbine aerodynamic performance represents a focus of research. These researches include modifying airfoil shape parameters using genetic algorithm [11], coupling aerodynamic and structural objectives into Pareto selection [12], selecting the optimum value of five operating factors using the Taguchi method [13], and other special codes for optimization [14, 15]. The finite element method was applied for computational fluid dynamics with a structure interaction model [16]. However, this method does not relate extensive structure analysis for the study. The coupling of the aerodynamic and structural optimization was introduced for the design of HAWT blades [17]. ANSYS commercial software package was used in optimizing the blade structural design; by integration with WTBM wind turbine blade modeler, the computation time was 16 days [18].

VAWT blade structure optimization integrates the improvement of performance, economy, and structural integrity. Design parameters are interrelated, which requires complex optimization is recommended to solve the problem. Lamina stacking sequence

is optimized by integrating finite element analysis and genetic optimization algorithm. The model constraints are buckling analysis, modal analysis, blade deformation, and stress distribution. The objective is weight reduction over the ELECTRA 30 kW existing model [19]. The presented model achieved a weight reduction of 17.4%, and the final weight is 228 kg. Another approach to optimize a beam weight, fundamental frequencies, and the total cost used the particle swarm algorithm for optimization of hybrid composite material structure. The approach includes the parameters thickness, orientation, volume fraction, matrix and fiber material used, and the number of laminae [20]. Moreover, the genetic algorithm is deployed in solving the problem of composite lamina stacking sequence [21] and the harmony search algorithm [22]. The concept of cost normalizing to unbind the cost from currency exchange and price changes was introduced by [23] as a material comparison. However, this concept could have enhanced optimization model efficiency.

Research on structure design and optimization investigates the VAWT structure integrity, life, and durability. However, theoretical investigations are not accurate compared to experimentation. Hence, a validation and conforming procedure are introduced to ensure the durability of the VAWT structure and to prevent any further hazards due to sudden structure failure. The procedure is called ultimate load tests including dynamic crash, and uniformly distributed static load tests, which could experimentally determine the maximum working condition and load [24].

Concluding, the literature survey shows that blade design is constrained to manifold design aspects and affected by discordant parameters. Moreover, the previous research did not focus on time and computation resources, besides the lack of addressing a variety of design parameters and variables for blade design. Consequently, the blade design optimization challenge is focused on interrelated variables and interchangeable design alternatives; furthermore, the focus is on computational improvement; those are the aims of the presented approach.

The study emerges the objectives of COP27 and the concept of sustainable designs by introducing structural optimization for device harvest energy from renewable source. Nowadays, the need for having renewable energy source in residence and houses is growing quickly, to enable such idea the design stage should be shorten, flexible, and efficient. VAWT has great potential to be an adaptable residence renewable energy device. The structural optimization approaches introduced herein could be used in improving the design of VAWT to wide their usage economically and efficiently.

This paper addresses and solves the challenges of blade design optimization. The aim is to presents a novel approach to reduce time and computation resources. As well as it covers various design parameters and variables. This is done through augmentation of using an artificial intelligence search algorithm to improve the design efficiency and maintain better behavior. The approach novelty is the hypothesis for analysis and employment of an empirical method for estimating the geometric cross-sectional properties. Regarding the cost objective, the concept of the cost index of the material selection tradeoff is developed. The current paper is limited to the static analysis, design and optimization. The dynamic effects are not considered herein.

The paper is arranged such as blade design parameters are discussed including the loading, geometric and material aspects. The parameterization section focuses on the

load analysis hypothesis, composite material parameters and limitations, the cost indexing, and the cross-sectional geometric properties and then the optimization models formulation, introducing the concept of genetic algorithm. The method of introducing the design parameterization into the optimization model and the embedding of the genetic algorithm are discussed in the optimization section. The results' discussion starts with ANSYS comparison to the presented approach; then, the results are compared to the ANSYS for validation. After that, the comparison between the four optimization models is discussed.

Blade design parameterization

Vertical-axis wind turbine blades are designed to sustain working and operating conditions. According to cited publications, and design codes, these conditions are operation in normal and maximum wind speeds, parking condition, sudden stop, and starting condition. In this section, the blade design aspects and parameterization are discussed. The parameters include the geometric properties, the material specification, and the loads applied on the blade. The blade parameters are shown in Fig. 1 including the lamina design parameters, the rotation angle (ω), and the rotor radius (R).

Geometric parameters

There are three common cross-sectional configurations: shell with no, single, or double shear webs. Consequently, the design parameters will vary according to the proposed design. Structure with shear web(s) requires extra design parameters to define the optimum location of the shear web(s). The web thickness could be varying also, which requires addressing extra parameters to the optimization model.

Geometric cross-sectional properties used in the current model include the cross-sectional area, first and second moment of area, polar moment of area, the center of mass, and aerodynamic center. The approach depends on the estimation of these values

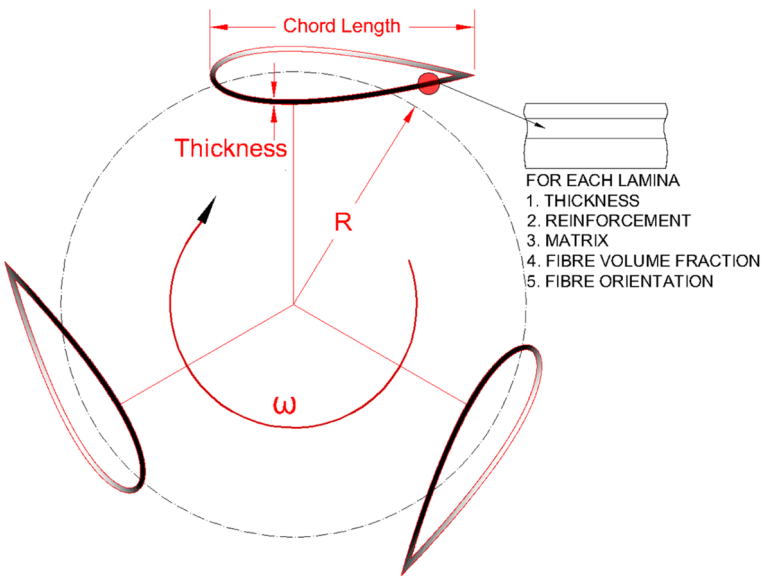

Fig. 1 The parameters of VAWT and the blade

by an empirical formula for every airfoil designation. Figure 2 shows the variation of the selected geometric properties for NACA 0021 against the thickness domain according to the shape constraint. The empirical formulas are polynomial equation, the equation degree depends on the properties to be estimated, and the empirical formula used for cross-sectional area is second degree polynomial function.

Material parameters

Blades under consideration are made from different forms of composite laminate material, as shown in Tables 1 and 2. The investigated structure is of unidirectional angled lamina type. Besides, the approach presents four investigation models. The first model material parameters are lamina thickness and fiber orientation. The second model material parameters are fiber material, lamina thickness, and fiber orientation. The third model material parameters are volume fraction, lamina thickness, and fiber orientation, while the fourth model material parameters are fiber material, matrix material, volume fraction, lamina thickness, and fiber orientation.

The parameters introduced for each design scenario are interrelated and have variables' limitations. Based on manufacturing restrictions, the thickness should be constrained to the lamina thickness and should be determined as the number of sub-laminae in each lamina, to mimic the manufacturing methods. Due to the production techniques, the preferred orientation angles measured from the z-axis are 0°, ±30°, ±60°, and ±90°. Furthermore, the conditions of maximum and minimum volume fraction impose limits on it.

Loading parameters

The aerodynamic load comprises the main external force affecting the blade. The study considers the resultant effective load at the aerodynamic center, in the form of tangential, normal, and moment as a function in azimuth angle. Figure 3 shows the fluctuation of aerodynamic loads in respect to azimuth angle changes and wind speeds; observing the maximum and minimum loads are occurring at a limited number of angles as marked in the figure for the maximum loads, the aerodynamic data is extracted from [26]; the turbine parameters are typically shown in Table 3. The selection of maximum and minimum loads for each component leads to a limited number of load cases.

The normal wind condition states imply the range of operating speed, which affects the inertia load at the mass center. In addition, the inertia load is considered as the dominating static strength factor for the design evaluation. Inertia load depends on the rotations speed and the blade mass which results in a high centrifugal load. The deformation due to inertia load is higher than the aerodynamic load, where the design of the blade depends on the surviving the inertia load in the static evaluation [6, 10, 24].

Methods

The proposed models are concerned with minimizing blade weight and cost index while maintaining the constraints of geometric and structural safety. The formulation of the optimization model depends on the sub-models for evaluating the mass, the cost index, the strength, and the geometric characterization. The optimization model is formulated according to the characteristics and nature of design parameters, decision variables, and

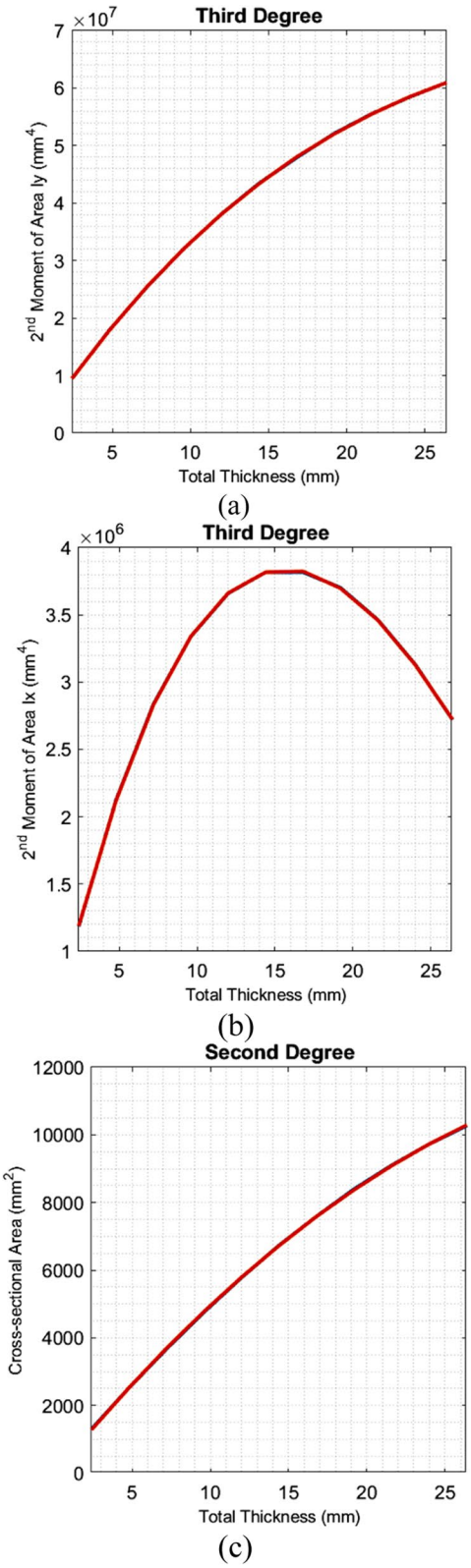

Fig. 2 Curve fitting empirical formula for selected geometric properties. **a** and **b** are the second moment of area at *y*-axis and *x*-axis respectively; the formula is third-degree order; **c** is the cross-sectional, area and the formula is second-degree order

Table 1 Lamina material's properties extracted from (ANSYS documentation)

Type	E_1	E_3	G_{12}	G_{23}	υ_{12}	ρ	C	t
Epoxy/carbon	121	8.6	4.7	3.10	0.27	1490	110	0.5
Epoxy/E-glass	45	1.0	5.0	3.85	0.3	2000	15	0.6
Epoxy/S-glass	50	8.0	5.0	3.85	0.3	2000	25	0.6
Unit	GPa	GPa	GPa	GPa	-	kg/m^3	-/m^3	mm

Table 2 Fiber and resin materials' properties extracted from (courtesy [25])

Type	E_1	G_{12}	υ_{12}	s_1	T_1	ρ	C	t
E-glass	72	38	0.4	2400	2400	2600	30	0.6
S-glass	85	39	0.4	4500	4500	2500	50	0.6
Aramid	4	6	0.4	3.6	3.6	1500	80	0.6
HS carbon	253	18	0.3	4500	4500	1800	150	0.5
Polyimide	3.45	0.13	0.5	70	89	1218	13	-
Polyester	4	0.24	0.5	80	80	1250	11	-
Epoxy	4.5	0.27	0.4	130	130	1320	15	-
Units	GPa	GPa	--	MPa	MPa	kg/m^3	-/m^3	mm

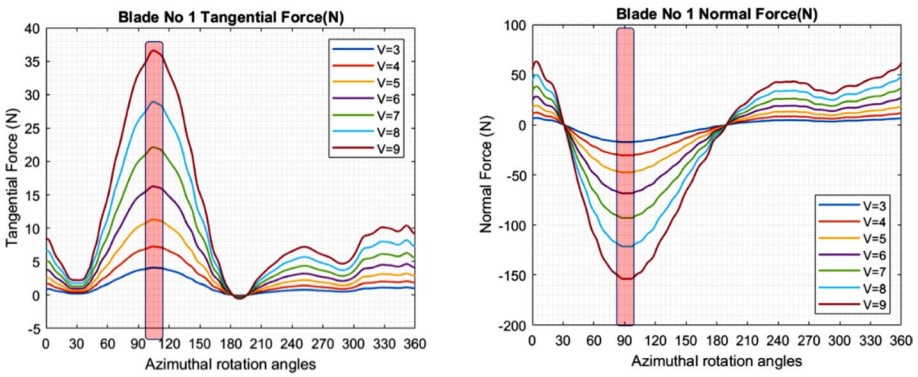

(a) Tangential force (b) Normal force

Fig. 3 Aerodynamic load fluctuations

Table 3 Wind turbine parameters and operating conditions

Parameter	Value
Blade length	1200 mm
Method of fixation	2 supports at a fourth of the length
Arm radius	1000 mm
Airfoil designation	NACA 0021
Chord length	265 mm
Tip speed ratio	2.58

constraints/objective functions. The model is then a multi-objectives model; consequently, the Pareto frontier concept will be used.

The algorithm employs in this study is the elitist genetic algorithm. It is a variant of the non-sporting dominated genetic algorithm II (NSGA II) [27]. Figure 4 shows the flow chart of the optimization model used in the presented approach. The elitist GA favors individuals with better fitness value by ranking the individuals for selection. A controlled elitist GA differentiates between individuals to adopt who can increase the population diversity even if they have a lower fitness value. The crucial point herein is maintaining population diversity for convergence to an optimal Pareto Frontier. The algorithm stops if the spread, a measure of the movement of the Pareto Frontier, is small.

The algorithm uses four layers for producing a new population: selection, crossover, mutation, and migration criteria. Selection is the process of choosing the fit candidates and rejecting others. Then, to add randomity to the solution and to avoid the local optimum trapping, the new population is generated by mixing the selected individuals. Crossover is the mixing between individuals while mutation is random flipping to the new individuals. After a range of iterations, the previous optimum solutions are migrated to the solution candidate to improve the algorithm efficiency. The number of populations is 200, the number of generations is 500, the Pareto fraction is 40%, distance measuring is distance crowding, and the stopping criterions based on fitness tolerance. The optimization model needs the identification of decision variables, objective functions, and constraints.

The decision variables (*D. V*) represent the blade design parameters. The decision variables assigned for the optimization model is as follows:

$$D.V : \{x\} \in [\{P\}\{D\}]$$

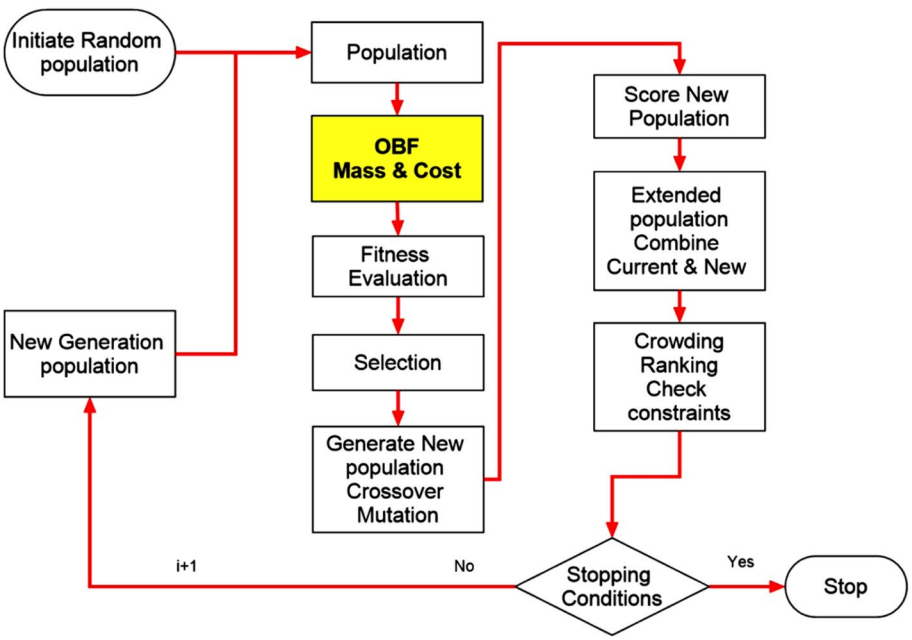

Fig. 4 Flowchart for the multi-objective optimization model in the study using elite genetic algorithm

Table 4 Decision variables {*P*} for composite structure parameters

DV	Unit	Type	Mapping	Model
tI	--	Integer	$x_1 - x_N$	A-D
OI	--	Integer	$x_{N+1} - x_{2N}$	A-D
MI	--	Integer	$x_{2N+1} - x_{3N}$	A-D
FI	--	Integer	$x_{3N+1} - x_{4N}$	D
VF	%	Continues	$x_{4N+1} - x_{5N}$	C-D

Table 5 Decision variables {*D*} shear web geometric design parameters

DV	Unit	Type	mapping	Model
X_{w1}	mm	Continues	y_1	1-4
X_{w2}	mm	Continues	y_2	1-4

Concluding from the parameterization section, the decision variables depend on the parameterization of blade design models. Hence, the decision variables are categorized into {*P*} and {*D*} representing the composite structure design parameters and cross-section design parameters, respectively. Material parameters depend on the investigated models. The first model has constant lamina material properties altering the thickness and the orientation only; thus, {*P*} include lamina's thickness and the fibers' orientation variables. The second model varies the lamina material properties, then {*P*} will include besides the first model variables, the material selection index. Cross-sectional design parameters {*D*} include the location of first and second shear webs; those are determined according to the proposed model; the decision variables {D} is considered for the four models.

Continues decision variables are *VF* representing fiber volume fraction assigned to the third and fourth approaches and X_w the location of the shear web(s) from the tip of the airfoil the variable is assigned for the second and third categorical cross-section design. The X_w is considered a design parameter {*D*}, while *VF*is considered a composite material parameter {*P*}, as listed in Tables 4 and 5.

Integer decision variables represent selection indexes and the number of sub-laminae. The *tI* is the number of sub-laminae, and it is assigned for all the approaches. The *OI* is the index of selected orientation angle and assigned for all the approaches. The *FI* and *MI* are the index of selected material, where *F* and *M* stand for fiber and matrix material selection respectively, and they are assigned for the third and fourth approaches. However, in the second approach, the *MI* is used as a lamina material index.

The objective functions minimize both the blade mass and the cost index. The represented objective functions are considered nonlinear, which depends on the geometric cross-section and material properties as expressed in Eq. (1). Figure 5 describes the dependence of objective functions on thickness, lamina number, and material parameters but does not depend on orientation angle, where this parameter is exclusive for constraint functions only.

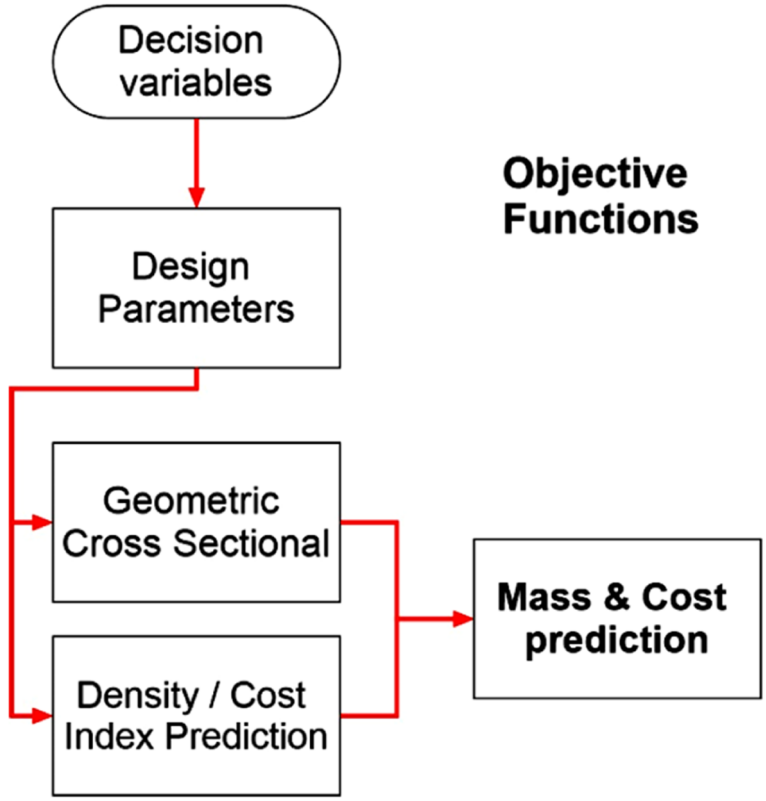

Fig. 5 OBF flowchart

$$OBF(\lceil x \rceil) = \min \begin{cases} \sum_{i=1}^{n} \rho_i V_i \\ \sum_{i=1}^{n} C_i \rho_i V_i \end{cases} \tag{1}$$

The ρ is the lamina density (kg/m^3), V is the lamina volume m^3, and C is the lamina cost index.

Three constraints categories bound the solution of the optimization problem. The first category is the search domain limits that represent the bounds of every decision variable. These bounds depend on the description of the design problem. The OI is an integer and represents the index of selected angles from proposed angles. The FI and MI are integer and represent the index of fiber and matrix material, respectively. Equation (2) shows the bound constraints.

$$S.T. \begin{cases} tI_{min} \leq tI \leq tI_{max} \\ OI_{min} \leq OI \leq OI_{max} \\ FI_{min} \leq FI \leq FI_{max} \\ MI_{min} \leq MI \leq MI_{max} \end{cases} \tag{2}$$

The second category is the nonlinear failure criteria vector constraint functions (F) the value should not exceed or equal to one as condition of failure (Fig. 6). The third category is the shape and the geometric dependence. The structural hypothesis is plane stress; hence, the total thickness to length (t/L) should be less than 1:15for the consideration of classical lamination theory [25]. The fiber volume fraction (VF) is bounded

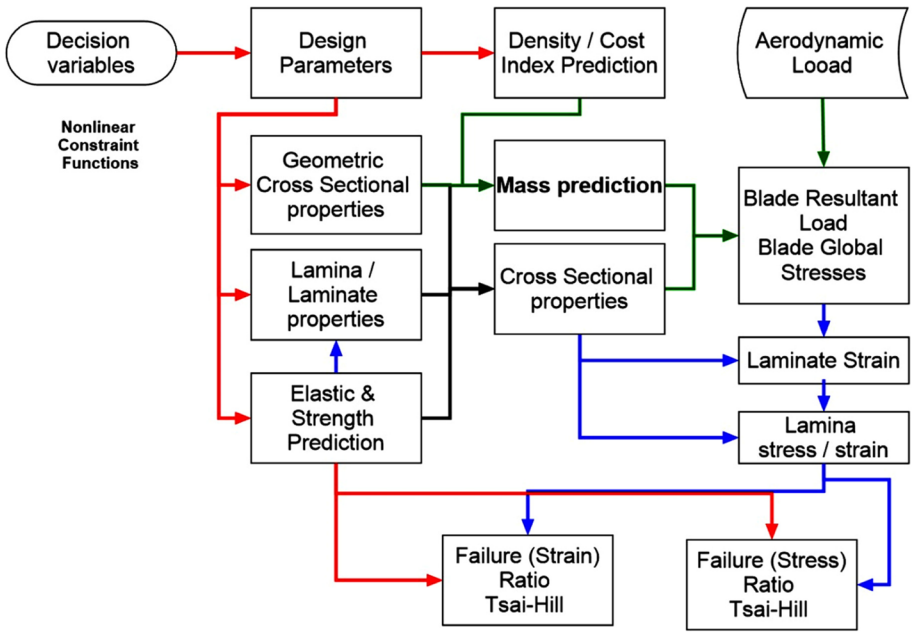

Fig. 6 Evaluation proposed design against failure flowchart

between 20 and 80% as the effective range according to recommendation of fiber volume fraction [25]; Eq. (3) shows the continuous constraints.

$$S.T.\begin{cases} t/L < 1/15 \\ [F] < 1 \\ 0.2 \leq VF \leq 0.8 \end{cases} \tag{3}$$

Results and discussion

The simulation and optimization of VAWT blade, with straight uniform cross-section and NACA four digits symmetric outer profile, is evaluated using the presented optimization approach. The blade structure is made from laminate composite material. The scope is to reduce the weight and the cost while maintaining structure safety and integrity. The blade design is dominated to load due to inertia in the static stresses, which requires reduction of the weight and maintaining the geometric properties in acceptable ranges for the concern of stress distribution. The blade failure is considered for first lamina failure; failure criteria are used to examine the safety due to stresses and strains. Moreover, the failure due to quadratic modified theory such as Tsai-Hill and Tsai-wu is also considered. The optimization of blade structure uses genetic algorithm; the method used is invariant of NSGA-II which is called elite genetic algorithm. Optimization parameters adopted in this study are found in Table 6. The platform of the study is MATLAB 2020; rather than that, the default values are used.

Model A shows an optimum blade design with a mass of 2.9 kg and 57.6 cost index, where blade design has the orientation of [60/135/30/180]° and thickness 0.6 for all laminae. However, all the results on the Pareto are optimum; the upper front solution

Table 6 Optimization algorithm parameters

Parameter	Value
Population number	*200*
Number of generations	*500*
Pareto front fraction	*40%*
Distance measuring method	*Crowding*
Stopping criteria	*Fitness tolerance 1e-6*

is selected for comparing the results of every model with each other. Figure 7 shows the Pareto plot for model A. The ANSYS-ACP has the capability of optimizing the same problem using the NSGA II genetic algorithm; however, the method takes a long time, and there is a limitation on the optimization method to the present method only. The presented approach shows promising performance in comparison to the ANSYS model; Table 7 shows a brief comparison between ANSYS-MOGA and model A. The created model consists of five integrated sub-models over ANSYS 16 workbench. ANSYS model flow chart is shown in Fig. 8. Model A shows only one optimum solution, because in this model, the cost and mass are considered depending due to the lack of material alteration. Consequently, in this case, a single objective function is preferred.

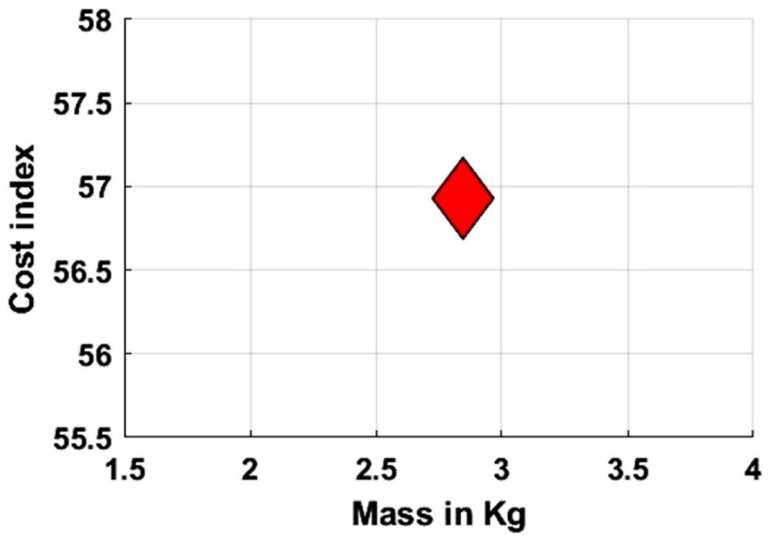

Fig. 7 Model A Pareto front

Table 7 ANSYS and approach A optimization comparison

Item	ANSYS	Approach
Computation time (hour)	172	< 1
Pareto frontier feature	Yes	Yes
Genetic algorithm	Yes	Yes
Algorithm control options	No	Yes
Hybrid optimization	No	Yes
Optimum mass	3 kg	2.9 kg
Optimum cost index	~58	~58

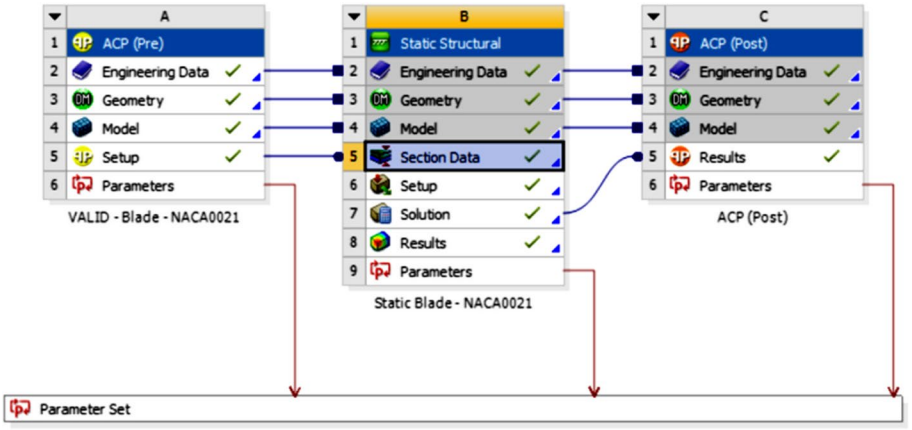

Fig. 8 ANSYS flow chart

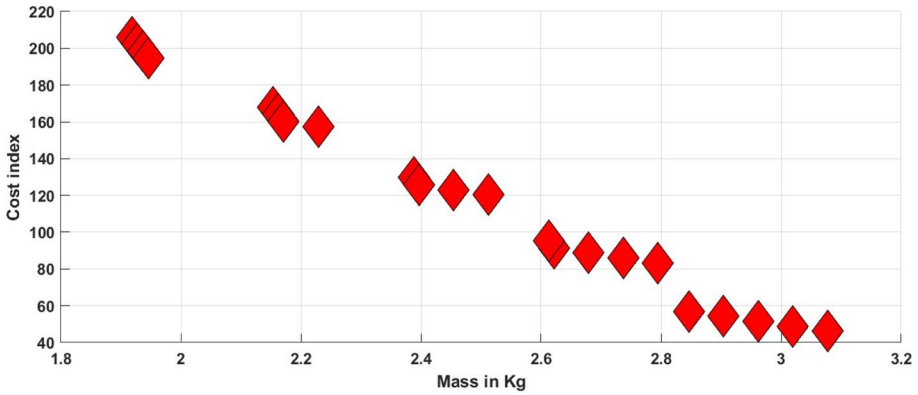

Fig. 9 Model B Pareto front

Model B Pareto front is shown in Fig. 9. The range of optimum designs' masses is from 3.1 to 1.9 and the cost index from 46 to 230. The optimum design selected which is the Pareto front one in the rank has a mass of 2.9 kg and a cost index of 95. The optimum design has lamina's thickness of [0.6/0.5/0.6/0.6] and orientation [60/90/135/30]. This orientation is recommended by literature. The material selected in model B is S-glass/epoxy, carbon/epoxy, S-glass/epoxy, and S-glass/epoxy.

The optimum design from model C has a mass of 3 kg and a cost index of 68. The blade design is made from epoxy/E-glass laminate. Lamina thickness is constant and equal to 0.6 mm; the fiber volume fraction is constant along the laminae to be 50%. The orientation angles are [0/135/90/45]°. The design safety factors are 10.3 and 5.2 for the stress ratio and strain ratio, respectively. Figure 10 shows the Pareto front of model C. Model C shows only one optimum solution, because in this model, the cost and mass are considered depending due to the lack of material alteration.

The optimum design using model D has a mass of 2.5 kg and a cost index of 50, the design factor of safety 20 and 9.3 for stress ratio and strain ratio, respectively. The Pareto front plot is shown in Fig. 11.

The four models have a factor of safety that is very equivalent to the recommendation of wind turbine codes. The factor of safety is calculated using the ratio between the

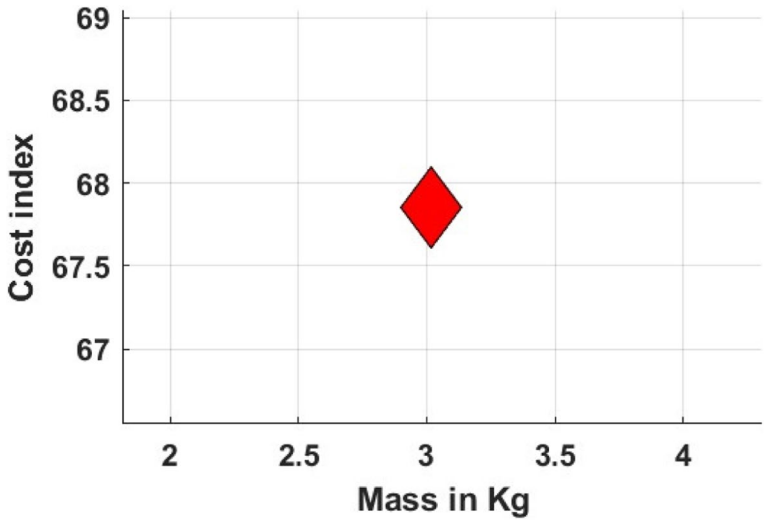

Fig. 10 Model C Pareto front

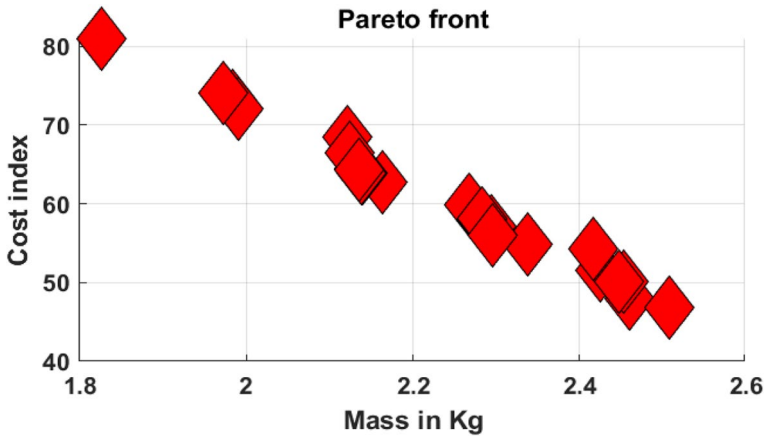

Fig. 11 Model D Pareto front

applied stress and ultimate stress for every lamina at maximum critical condition. Figure 12 shows the comparison of safety factors between the four models.

Concluding from results where the optimum preferable orientation angle would be the 90°, the dominant load shall be the inertia load as considered for critical load in the case of VAWT blade is centrifugal load. This orientation is preferable to maintain higher normal strength for the upper lamina; the results are concise with recommendations in [8, 24]. In order to calculate the cost index, Eq. (1) is used for every lamina in the design. Finally, the total cost index is the summations of all laminae cost indices.

Eventually, model A selects the optimum values of reinforcement orientation and the lamina thickness. These variables have a minor effect on mass and cost. Hence, the result shows less variation in the final optimum results, where all the optimum has the same cost index and mass. Otherwise, with the addition of other parameters, which is hybrid material laminate design, the result shows obvious variation in cost and mass on the Pareto front. Models A and B are based on stacking and thickness optimization for

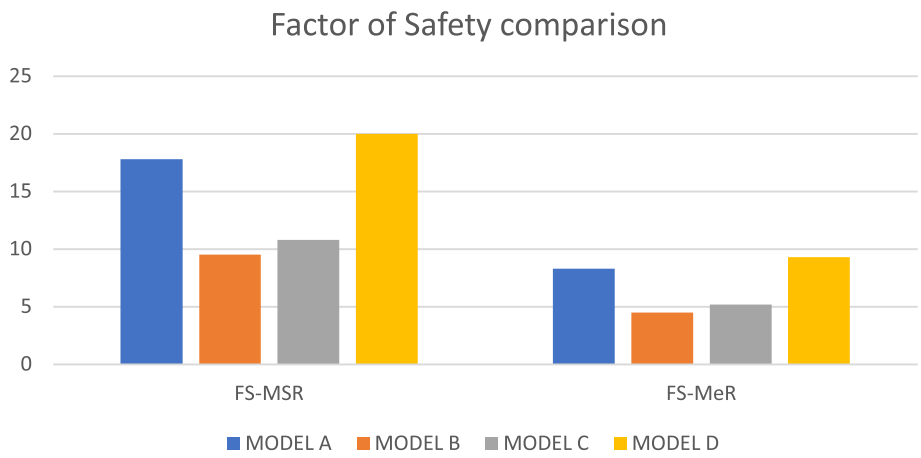

Fig. 12 Comparison of four models factors of safety

Table 8 Comparison between the four presented optimization models

Parameters	Model A	Model B	Model C	Model D
Cost index	58	95	69	50
Mass (kg)	2.9	2.8	3	2.5
Time (sec)	526	538	395	447
Lamina 1	E-glass/epoxy	S-glass/epoxy	E-glass/epoxy	E-glass/epoxy
Lamina 2	E-glass/epoxy	Carbon/epoxy	E-glass/epoxy	S-glass/epoxy
Lamina 3	E-glass/epoxy	S-glass/epoxy	E-glass/epoxy	S-glass/epoxy
Lamina 4	E-glass/epoxy	S-glass/epoxy	E-glass/epoxy	E-glass/epoxy
Thickness (mm)	[.6/.6/.6/.6]	[.6/.5/.6/.6]	[.6/.6/.6/.6]	[.6/.6/.6/.6]
Angle (deg)	[60/150/60/30]	[60/90/135/30]	[0/135/90/45]	[90/90/135/90]
Vf	[50/50/50/50]	[50/65/50/50]	[50/50/50/50]	[21/23/21/23]
FS-MSR	17.8	9.5	10.8	20
FS-MeR	8.3	4.5	5.2	9.3

laminate design and do not include the variation of lamina properties such as the volume fraction and lamina composite materials. Models C and D focus on the lamina properties. They include the volume fraction and the variation of reinforcement and matrix materials. Comparison between the four models is presented in Table 8.

The lamina thickness depends on the number of sub-laminae in the single lamina; hence, the approach assumes that every lamina could consist of a single lamina up to four laminae. However, the final optimum results shown in Table 8 shows lamina of single sub-lamina. This is clear in the case of 0.6 thicknesses for E-glass and 0.5 for carbon lamina.

Conclusions

Vertical-axis wind turbine, with straight uniform cross-section and NACA four digits symmetric outer profile, is evaluated using the presented optimization approach. The blade is made from laminate composite material. The scope is to reduce the weight and the cost while maintaining structure safety and integrity. The blade design is

dominated to load due to inertia in the static stresses, which requires reduction of the weight and maintaining the geometric properties in acceptable ranges for the concern of stress distribution. The blade failure is considered for first lamina failure; failure criteria are used to examine the safety due to stresses and strains. Moreover, the failure due to quadratic modified theory such as Tsai-Hill and Tsai-wu is also considered.

Stress/strain distributions depend on the lamina mass and the geometric cross-sectional properties. Consequently, the dominant load is the inertia load. This is noticeably clear in final optimum results where the optimum preferable orientation angle would be the 90°. This orientation is preferable to maintain higher normal strength for the upper lamina, same as recommended in [8, 24]. However, the optimization model shows preferable angles; structural analysis shows that the design is dominated by inertia.

The approach mimics reality in the design and manufacturing from the aspect of thickness variation and altering the orientation angel. The lamina thickness depends on the number of sub-laminae in the single lamina; hence, the approach assumes that every lamina could consist of a single lamina up to four laminae. The number of laminae in the laminate is constant and not included as a variable to have a fixed chromosome length where every variable vector has a fixed length along with the optimization. The genetic algorithm is more efficient in optimizing the composite lamina design for complex shapes and loading conditions; thus, several design parameters are included adding more alternatives to have higher efficiency from the optimization model and achieve more optimum results. The study of comparing the capability of the genetic algorithm was studied by introducing the mentioned optimization approaches.

The approaches' results were studied to determine which could be better in tailoring the optimum design. Model A considers the lamina is predefined and its properties are invariant and hence concerned about altering the stacking design including thickness and orientation. Model B is remarkably similar to the first one yet adding the variability of the lamina, where material selection is to determine the lamina material from a list of four different ones. Model C is concerned about tailoring the lamina properties yet for single fiber and matrix material in addition to altering the stacking sequence; hence, this approach is considered as hybrid lamina invariant constitution materials. The fourth approach considers the concept of hybrid laminate, by selecting fiber material, matrix material, and volume fraction for every lamina, besides the selection of stacking design parameters including thickness and orientation. Eventually, model D shows better performance compared to the other three models, because of the flexibility to tailor the lamina properties according to the application and loading conditions. The final optimum results show the mass range between 2.5 and 3 kg, and the cost index varies from 40 to 90, depending on the material used.

The computation efforts needed to examine more alternatives and enormous optimum solutions were considered in the study. Consequently, intrinsic implementation of an algorithm to search for the most dangerous locations shows a high potential to reduce computational time and cost. This algorithm enables the optimization module to limit the constraint functions to check for fewer locations rather than applying the genetic algorithm for the whole structure and the entire loading conditions.

Moreover, the usage of empirical approximate formulas to evaluate the geometric properties avoids the usage of finite element codes in the optimization algorithm, reducing the computation time and cost.

The approach novelty is the empirical formulas that evaluate the geometric properties and pre-preparation algorithm to confine the searching space and reduce the time. They expand the optimization model capabilities for finding better optimum design. The proposed approach still needs integration with an acceptable life prediction model to enhance the optimum results and to be more comprehensive. Furthermore, the requirement to evaluate the four models by extending the study to include progressive failure and interlaminar stress/strain distribution, besides the inclusion of the stresses as objective functions, could improve the design.

Nomenclature

$\{D\}$ Design decision variables
$\{P\}$ Material structural decision variables
X_{w1} Location of the first shear web
X_{w2} Location of the second shear web
E_1 Modulus of Elasticity in the longitudinal direction
FS-MeR Factor of safety for the maximum strain ratio criterion
FS-MSR Factor of safety for the maximum stress ratio criterion
G_{12} Modulus of rigidity in the main plane
G_{23} modulus of rigidity in traverse plane
S_1 Strength in the longitudinal direction
t Lamina thickness
T_1 Shear strength
FI Fiber material selection index
MI Material selection index
OI Fiber orientation index
VF Fiber volume fraction
tI Number of laminae in each laminate
$\boldsymbol{C}$ Cost index/m^3
ρ Density in kg/m^3
v_{12} Major Poisson's ratio

Abbreviations

GA	Genetic algorithm
HAWT	Horizontal axis wind turbine
HS	High strength
IEC	International electro-technical commission
NACA	National Advisory Committee for Aeronautics
NSGA	Non-sorting dominated genetic algorithm
VAWT	Vertical-axis wind turbine
MOGA	Multi-objective genetic algorithm
MOBF	Multi-objective functions
SOBF	Single objective function

Acknowledgements
Not applicable

Authors' contributions
A. Genied as 1st author wrote the paper, designed the models, and analyzed the results using Matlab and ANSYS. M. Attia and A. Badawy as the 2nd and 3rd authors helped in analyzing the results, suggested modifications to the models, and then approved the paper. The authors read and approved the final manuscript.

Funding
No funding was obtained for this study.

Availability of data and materials
The data used in this research can be found via the corresponding author.

Declarations

Competing interests
The authors declare that they have no competing interests.

Received: 10 May 2022 Accepted: 25 September 2022
Published online: 01 October 2022

References

1. Tummala A, Velamati RK, Sinha DK, Indraja V, Krishna VH (2016) A review on small scale wind turbines. Renew Sust Energ Rev 56:1351–1371. https://doi.org/10.1016/j.rser.2015.12.027
2. Toja-Silva F, Lopez-Garcia O, Peralta C, Navarro J, Cruz I (2016) An empirical–heuristic optimization of the building-roof geometry for urban wind energy exploitation on high-rise buildings. Appl Energy 164:769–794. https://doi.org/10.1016/j.apenergy.2015.11.095
3. Balduzzi F, Bianchini A, Carnevale EA, Ferrari L, Magnani S (2012) Feasibility analysis of a Darrieus vertical-axis wind turbine installation in the rooftop of a building. Appl Energy 97:921–929. https://doi.org/10.1016/j.apenergy.2011.12.008
4. Eriksson S, Bernhoff H, Leijon M (2008) Evaluation of different turbine concepts for wind power. Renew Sust Energ Rev 12(5):1419–1434. https://doi.org/10.1016/j.rser.2006.05.017
5. Blanco MI (2009) The economics of wind energy. Renew Sust Energ Rev 13(6-7):1372–1382. https://doi.org/10.1016/j.rser.2008.09.004
6. Raciti Castelli M, Dal Monte A, Quaresimin M, Benini E (2013) Numerical evaluation of aerodynamic and inertial contributions to Darrieus wind turbine blade deformation. Renew Energy 51:101–112. https://doi.org/10.1016/j.renene.2012.07.025
7. Deng W, Yu Y, Liu L, Guo Y, Zhao H (2020) Research on the dynamical responses of H-type floating VAWT considering the rigid-flexible coupling effect. J Sound Vib 469. https://doi.org/10.1016/j.jsv.2019.115162
8. Hameed MS, Afaq SK, Shahid F (2015) Finite element analysis of a composite VAWT blade. Ocean Eng 109:669–676. https://doi.org/10.1016/j.oceaneng.2015.09.032
9. Lin J, Xu Y-l, Xia Y (2019) Structural analysis of large-scale vertical axis wind turbines part II: fatigue and ultimate strength analyses. Energies 12(13). https://doi.org/10.3390/en12132584
10. Hand B, Kelly G, Cashman A (2021) Structural analysis of an offshore vertical axis wind turbine composite blade experiencing an extreme wind load. Mar Struct 75. https://doi.org/10.1016/j.marstruc.2020.102858
11. Bedon G, De Betta S, Benini E (2016) Performance-optimized airfoil for Darrieus wind turbines. Renew Energy 94:328–340. https://doi.org/10.1016/j.renene.2016.03.071
12. Ferreira CS, Geurts B (2015) Aerofoil optimization for vertical-axis wind turbines. Wind Energy 18(8):1371–1385. https://doi.org/10.1002/we.1762
13. Chen W-H, Chen C-Y, Huang C-Y, Hwang C-J (2017) Power output analysis and optimization of two straight-bladed vertical-axis wind turbines. Appl Energy 185:223–232. https://doi.org/10.1016/j.apenergy.2016.10.076
14. Xu Y-L, Peng Y-X, Zhan S (2019) Optimal blade pitch function and control device for high-solidity straight-bladed vertical axis wind turbines. Appl Energy 242:1613–1625. https://doi.org/10.1016/j.apenergy.2019.03.151
15. Li C, Xiao Y, Xu Y-L, Peng Y-X, Hu G, Zhu S (2018) Optimization of blade pitch in H-rotor vertical axis wind turbines through computational fluid dynamics simulations. Appl Energy 212:1107–1125. https://doi.org/10.1016/j.apenergy.2017.12.035
16. Jafaryar M, Kamrani R, Gorji-Bandpy M, Hatami M, Ganji DD (2016) Numerical optimization of the asymmetric blades mounted on a vertical axis cross-flow wind turbine. Int Commun Heat Mass Transfer 70:93–104. https://doi.org/10.1016/j.icheatmasstransfer.2015.12.003
17. Dal Monte A, De Betta S, Raciti Castelli M, Benini E (2017) Proposal for a coupled aerodynamic–structural wind turbine blade optimization. Compos Struct 159:144–156. https://doi.org/10.1016/j.compstruct.2016.09.042
18. Maheri A (2020) Multiobjective optimisation and integrated design of wind turbine blades using WTBM-ANSYS for high fidelity structural analysis. Renew Energy 145:814–834. https://doi.org/10.1016/j.renene.2019.06.013
19. Wang L, Kolios A, Nishino T, Delafin P-L, Bird T (2016) Structural optimisation of vertical-axis wind turbine composite blades based on finite element analysis and genetic algorithm. Compos Struct 153:123–138. https://doi.org/10.1016/j.compstruct.2016.06.003
20. Megahed M, Abo-bakr RM, Mohamed SA (2020) Optimization of hybrid natural laminated composite beams for a minimum weight and cost design. Compos Struct 239. https://doi.org/10.1016/j.compstruct.2020.111984

21. Wei R, Pan G, Jiang J, Shen K, Lyu D (2019) An efficient approach for stacking sequence optimization of symmetrical laminated composite cylindrical shells based on a genetic algorithm. Thin-Walled Struct 142:160–170. https://doi.org/10.1016/j.tws.2019.05.010
22. Schaedler de Almeida F (2019) Optimization of laminated composite structures using harmony search algorithm. Compos Struct 221. https://doi.org/10.1016/j.compstruct.2019.04.024
23. Chen D, Sun G, Meng M, Jin X, Li Q (2019) Flexural performance and cost efficiency of carbon/basalt/glass hybrid FRP composite laminates. Thin-Walled Struct 142:516–531. https://doi.org/10.1016/j.tws.2019.03.056
24. Vergaerde A, De Troyer T, Carbó Molina A, Standaert L, Runacres MC (2019) Design, manufacturing and validation of a vertical-axis wind turbine setup for wind tunnel tests. J Wind Eng Ind Aerodyn 193. https://doi.org/10.1016/j.jweia.2019.103949
25. Kaw AK (2005) Mechanics of composite materials
26. Li QA, Maeda T, Kamada Y, Murata J, Furukawa K, Yamamoto M (2016) The influence of flow field and aerodynamic forces on a straight-bladed vertical axis wind turbine. Energy 111:260–271. https://doi.org/10.1016/j.energy.2016.05.129
27. Deb K, Pratap A, Agarwal S, Meyarivan T (2002) A fast and elitist multiobjective genetic algorithm: NSGA-II. IEEE Transact Evol Comput 6(2):182–197. https://doi.org/10.1109/4235.996017

Publisher's Note